Supplemental Figure 1. Age-related difference in tumor growth rate is eliminated in RAG-1^{null} mice. Growth curves of individual MC38 (A and D), B16 (B and E), 4T1 (C) murine tumors of young (red circles) and mature (blue squares) mice in Figure 1 are shown. Greater tumor growth rates in young WT mice (A-C) were not observed in RAG-1^{null} mice (D and E).

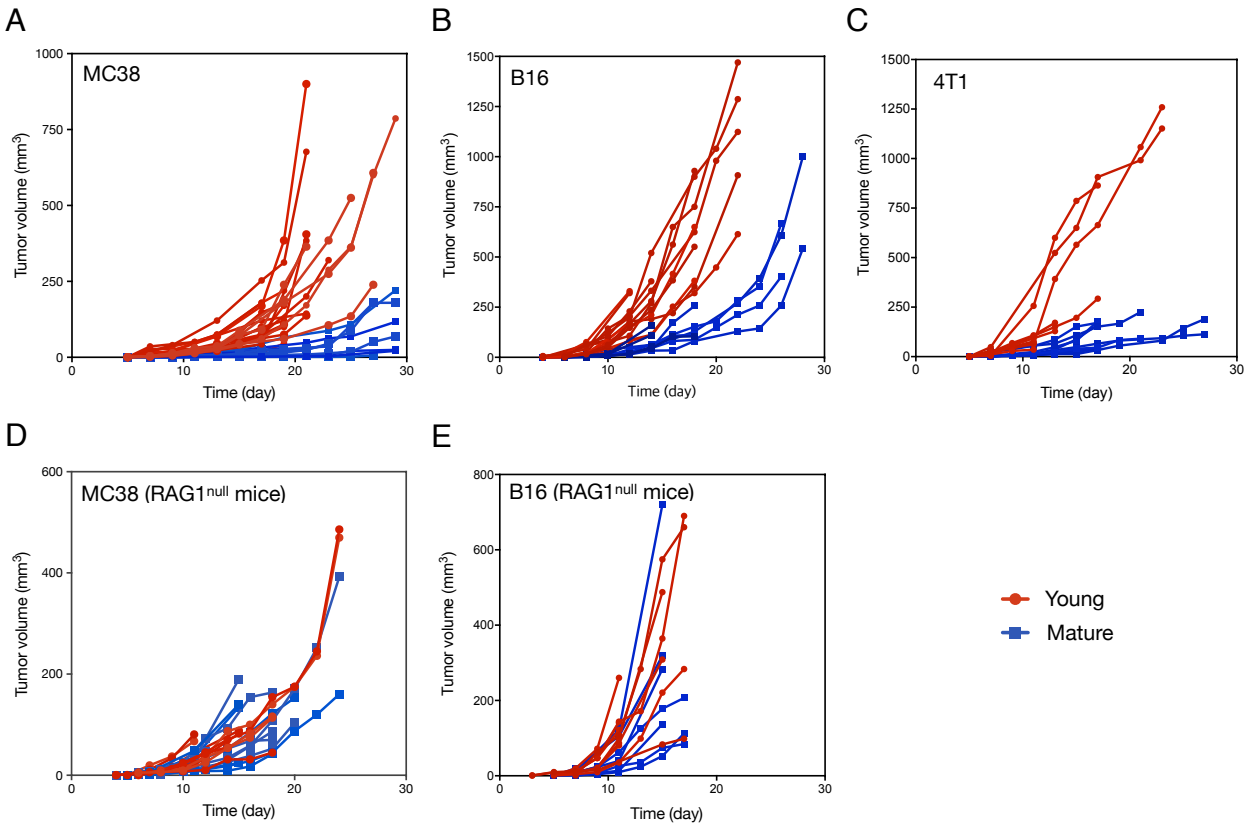

Supplemental Figure 2. *In vivo* CD8 depletion in tumor-bearing young and mature mice. (A) Schematic illustrating the experimental design of CD8 depletion in tumor-bearing mice. CD8 depletion in tumor tissues was confirmed by flow cytometry at day 14 of tumor growth in young (B) and mature (C) mice. Mice received anti-CD8 antibody treatment showed efficient depletion of $CD8^+$ T cell population among $TCR\beta^+$ cells as compared to mice received IgG isotype antibody.

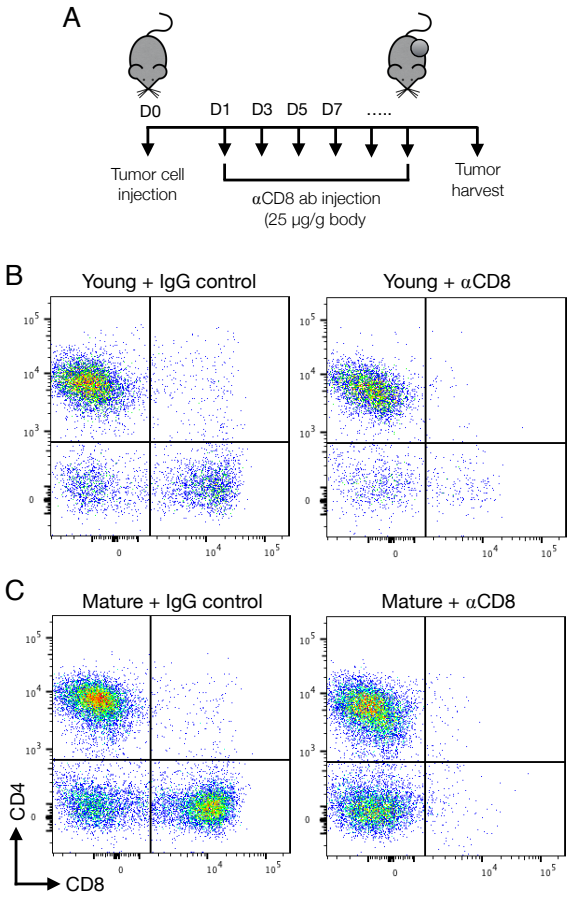

Supplemental Figure 3. CD49d expression level in T lymphocytes of spleen and peripheral blood of young and mature mice. Frequency of CD49d$^+$ cells and mean fluorescence intensity of CD49d were measured by flow cytometry in CD8$^+$, CD4$^+$, and CD4$^+$CD25$^+$FoxP3$^+$ regulatory T cells (T_{reg}). All data are plotted as means ± SEM. There was no statistical differences in the CD49d expression levels in the T cell populations of spleen or peripheral blood of young and mature mice (spleen: n=9-15; blood: n=5-9).

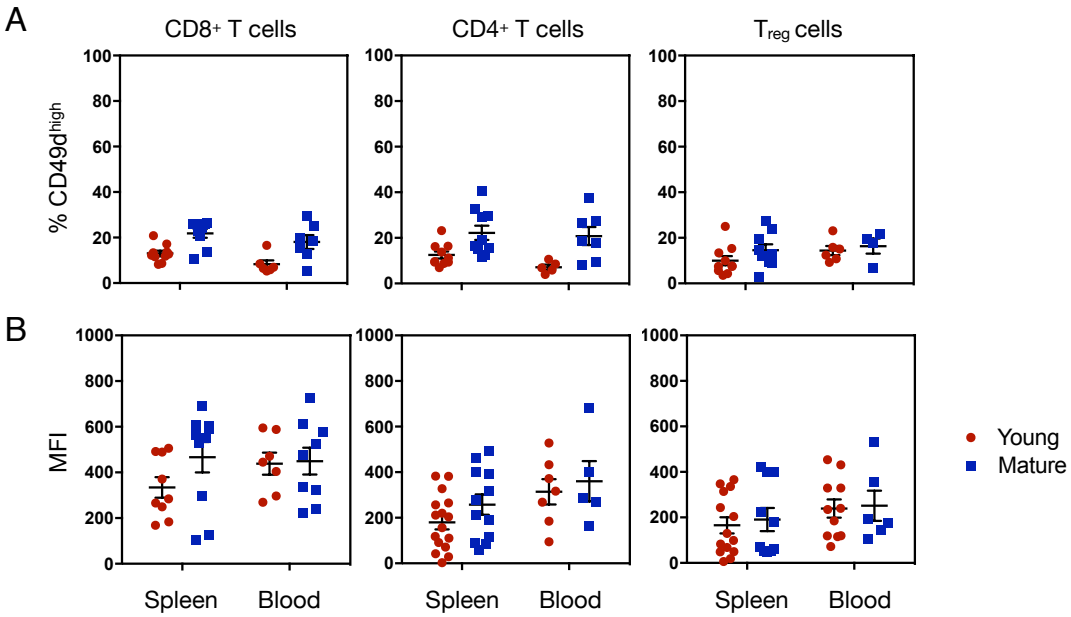

Supplemental Figure 4. ITGB1 (CD29) level in tumoral T cells of young and mature mice. Frequency of cells expressing ITGB1, β subunit of VLA4, in tumoral $CD8^+$ (A), $CD4^+$ (B), and $CD25^+$ $FoxP3^+$ regulatory T cells (C) of young and mature mice was measured by flow cytometry. Frequency of $CD29^+$ cells are compared to those of $ITGA4^+$ ($CD49d^+$) and VLA^+ ($CD29^+$ $CD49d^+$) cells. All data are plotted as means ± SEM. Two-way ANOVA was used for statistical analysis with correction for multiple comparisons by Turkey method (*P < 0.05, **P < 0.005, ***P < 0.0005, ****P < 0.00005; young: n=3; mature: n=6).

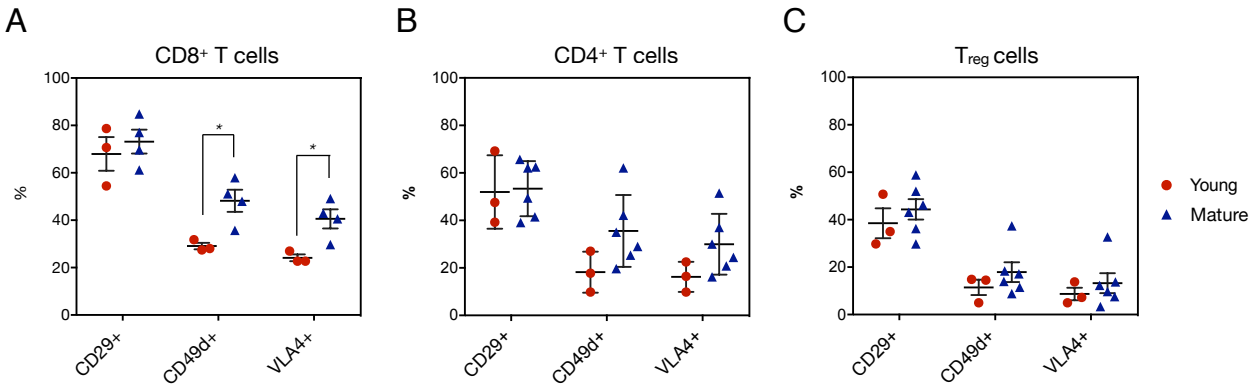

Supplemental Figure 5. Central memory T cell phenotype of intratumoral CD49d$^+$ and CD49d$^-$ CD8$^+$ T cells. Expression levels of CD44, (A) CD62L, and (B) CCR7 in tumor-infiltrating CD49d$^+$ CD8$^+$ and CD49d$^-$ CD8$^+$ T cells of mature mice were assessed by flow cytometry. EM: effector memory cell (CD44$^+$ CD62L$^-$ CCR7$^-$), CM: central memory cell (CD44$^+$ CD62L$^+$ CCR7$^+$). Each line of Before-after graphs represents individual tumor of mature mice. Paired *t*-test between CD49d$^+$ and CD49d$^-$ CD8$^+$ T cell subsets in each tumor did not show statistical significance (CD62L: n=7; CCR7: n=9).

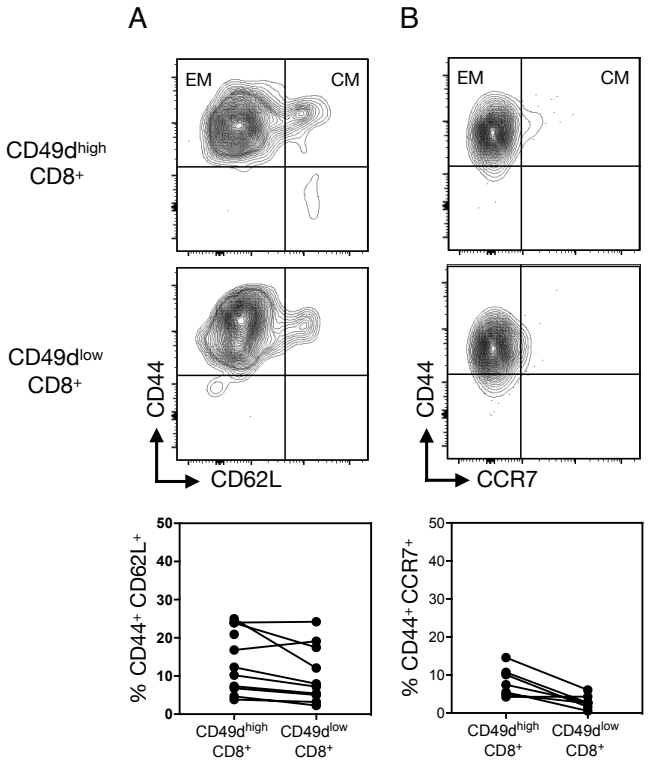

Supplemental Figure 6. Expression level of CD25 and CCR5 in tumor-infiltrating CD49d^{+} CD8^{+} and CD49d^{-} CD8^{+} T cells of mature mice. Paired *t*-test between CD49d^{+} and CD49d^{-} CD8^{+} T cell subsets in each tumor did not show statistical significance (CD25: n=4; CCR5: n=3). Data are plotted as means ± SEM.

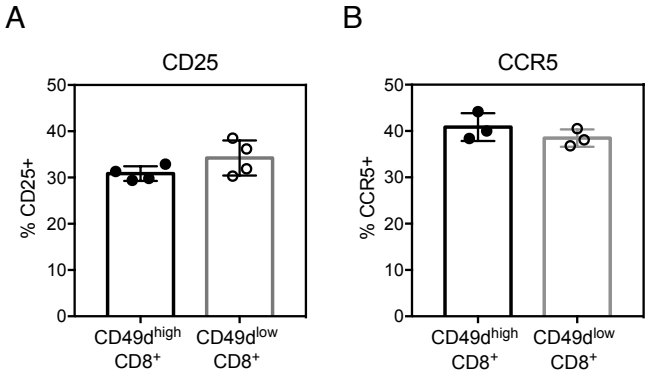

Supplemental Figure 7. Characterization of intratumoral CD49d$^+$ and CD49d$^-$ CD8$^+$ T cells of young mice. (A-D) Expression level of IFN-ɣ, granzyme B, Ki-67, and CD62L in tumor-infiltrating CD49d$^+$ and CD49d$^-$ CD8$^+$ T cells of young mice assessed by flow cytometry. Each line of Before-after graphs of panel A-C represents individual tumor. *P*-values were calculated based on the paired *t*-test between CD49d$^+$ and CD49d$^-$ CD8$^+$ T cell subsets in each tumor. (E) Linear regression analysis between the frequency of CD49d$^+$ CD8$^+$ T cells and and the number of infiltrating CD8$^+$ T cells in tumors of young mice. Each dot in panel E represents individual tumor samples.

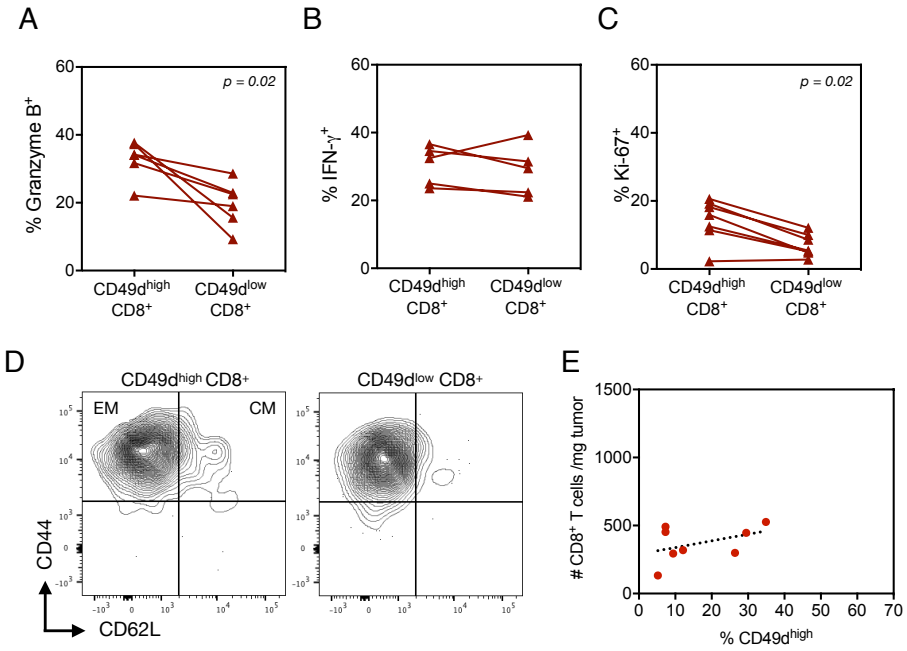

Supplemental Figure 8. Cell count of CD49d^{low} CD8^{+} cells in tumor tissues of young and mature mice at day 14 of tumor growth. All data are plotted as means ± SEM. *P*-value was calculated by Student's *t*-test (2-tailed). There was no statistical difference between two age groups (young: n=6; mature n=9).

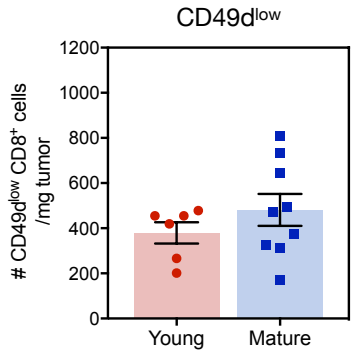

Supplemental Figure 9. Analysis of intratumoral macrophages and DCs of MC38 tumors of young and mature mice. (A) Expression level of CD49d (ITGA4) in tumor-infiltrating immune cell populations. MC38 tumors of young (red circle) and mature mice (blue square) were harvested on day 10 of tumor growth and assessed for frequency of CD49d^{+} cells among CD8^{+} T cells (CD45^{+} TCRβ^{+} CD8^{+}), CD4^{+} T cells (CD45^{+} TCRβ^{+} CD4^{+}), regulatory T cells (CD45^{+} TCRβ^{+} CD4^{+} FoxP3^{+}), tumor-associated macrophages (TAM, CD45^{+} CD11b^{+} F4/80^{+}), dendritic cells (DC, CD45^{+} CD11c^{+} MHCII^{high}), and neutrophils (CD45^{+} CD11b^{+} Ly-6G^{+}) by flow cytometry (n=5-12 per group). Transcriptome analysis of tumor-infiltrating TAMs (B) and DCs (C) by RNA-seq. Differentially expressed genes in DCs of young mice and mature mice (FDR < 0.05) are labeled in red dots and also represented in the heatmap. (D) Expression level of representative markers of M1 and M2 macrophages in TAMs of young and mature mice analyzed by RNA-seq. Markers for M1 are labeled in red, and markers for M2 is labeled in blue.

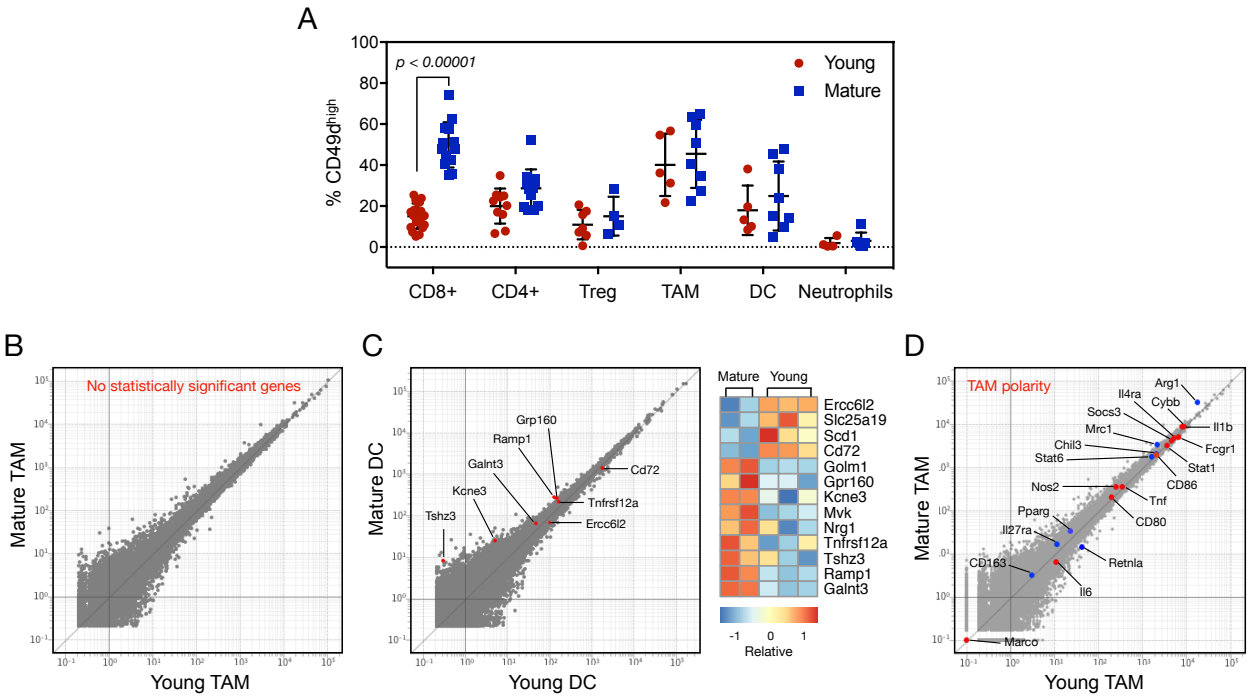

Supplemental Figure 10. Change in CD49d expression level in tumor-infiltrating T cells of young and aged mice with anti-VLA-4 antibody treatment. Frequency of CD49d$^+$ cells among tumoral CD8$^+$ (A), CD4$^+$ (B) and CD25$^+$ FoxP3$^+$ T cells (C) analyzed by flow cytometry. In both age groups, CD49d level on T cells was significantly reduced with anti-VLA-4 antibody treatment (green). All data are plotted as means ± SEM. For statistical test, two-way ANOVA was used with correction for multiple comparisons by Turkey method (*P < 0.05, **P < 0.005, ***P < 0.0005, ****P < 0.00005, n=9-12 per group).

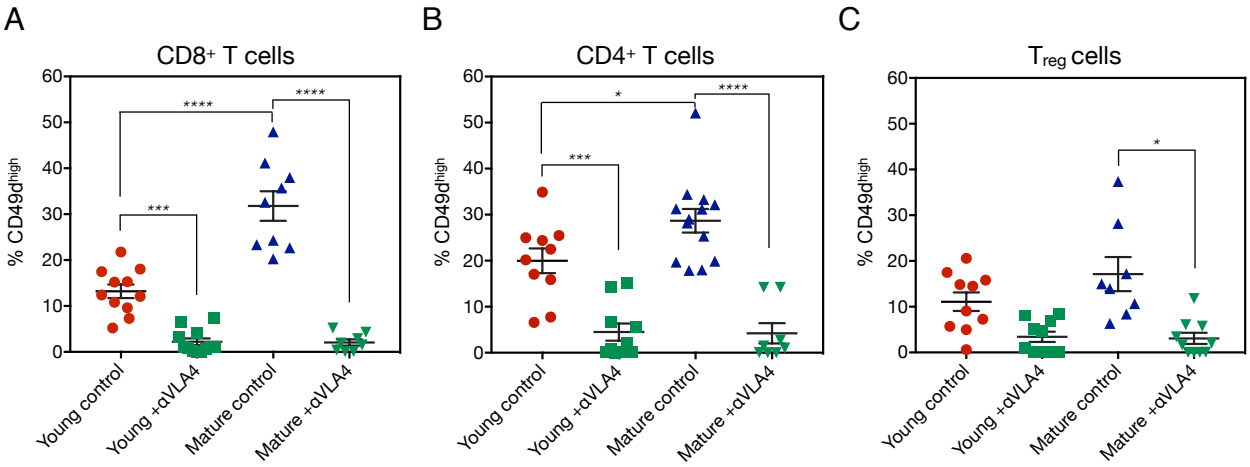

Supplemental Figure 11. Granzyme B level in tumor-infiltrating CD8$^+$ T cells of mature mice with anti-VLA4 antibody treatment. Cell frequency of granzyme B-expressing cells in total tumoral CD8$^+$ T cells of mature mice with or without treatment of anti-VLA-4 treatment was measured by flow cytometry (n=3). *P*-value was calculated based on Student's *t*-test (2-tailed).

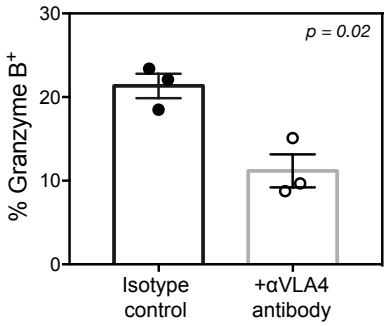

Supplemental Figure 12. Analysis of intratumoral TAMs and DCs of MC38 tumors of mature mice with or without anti-VLA-4 treatment. (A) Cell counts of intratumoral TAM, DC, and neutrophil of mature mice with anti-VLA4 antibody or IgG isotype treatment. (B) Expression level of MHC class II in TAMs of mature mice treated with anti-VLA4 antibody or IgG isotype. (n=5 each group).